Microchimica Acta
https://doi.org/10.1007/s00604-018-2822-6

ORIGINAL PAPER

Amperometric determination of As(III) and Cd(II) using a platinum electrode modified with acetylcholinesterase, ruthenium(II) -tris(bipyridine) and graphene oxide

Manju Bhargavi Gumpu[1,2] · Murugan Veerapandian[3] · Uma Maheswari Krishnan[4] · John Bosco Balaguru Rayappan[1,2]

Received: 20 December 2017 / Accepted: 29 April 2018

Abstract
The authors describe an amperometric biosensor for the determination As(III) and Cd(II) based on the inhibition of the enzyme acetylcholineesterase (AChE). A platinum electrode was modified with ruthenium(II)-tris(bipyridyl), graphene oxide and AChE and then showed redox peaks at 0.06 and 0.2 V vs Ag/AgCl in the presence of acetylthiocholine chloride (ATChCl). Amperometry unveiled a steady-state turnover rate with the release of thiocholine. In the presence of arsenic(III) and cadmium(II), AChE showed an inhibitive response at 0.214 and 0.233 V vs Ag/AgCl, respectively. The electrode exhibits a detection limit and linear range of 0.03 μM and 0.05–0.8 μM for As(III) and 0.07 μM and 0.02–0.7 μM for Cd(II), respectively. Type of inhibition and inhibition constants induced by As(III) and Cd(II) on the catalytic sites of AChE were determined from Dixon and Lineweaver-Burk plots. The modified electrode was applied to the determination of As^{3+} and Cd^{2+} in river, tap and waste water, and the results proved that the method is sensitive and can be an alternative to chromatographic and spectroscopic techniques.

Keywords Biosensor · Electron transfer · Competitive inhibition · Mixed inhibition · Dixon plot · Lineweaver-Burk plot · Ethylene diamine tetraacetic acid

Introduction

Arsenic (As) and cadmium (Cd) ions are major toxicants of the environment. To detect As(III) and Cd(II), enzyme inhibition based electrochemical biosensors were developed due to their distinctive advantages of high selectivity in the presence of enzymes, low cost of analysis, low consumption of reagents, lower detection limits and low power requirement [1]. Enzymes such as glucose oxidase [2], AChE [3–5], invertase and hydrogen peroxidase [6] have been utilized for inhibitive assay of ions such as Cd^{2+}, Pb^{2+}, Hg^{2+}, Zn^{2+} and Ag^{2+} [3, 7, 8]. However, there are very few reports on the detection of As^{3+} and Cd^{2+} ions at the AChE active sites and all these works were aimed in detecting either As^{3+} or Cd^{2+} ions. Kumar et al. [7] demonstrated the AChE reaction based stabilization of silver nanoparticles to determine Hg^{2+} ions based on fluorescence. However, this work is limited in studying the concurrent behavior of Pb^{2+} and Hg^{2+} ions and the selectivity of Pb^{2+} and Hg^{2+} is not well addressed with respect to thiophilic groups. To the extent of author's knowledge, no literature is available on the selective amperometric inhibitive assay of As^{3+} and Cd^{2+} ions. Amine et al. reported a review on biosensors based on enzyme inhibition highlighting cholinesterase as standard biocomponent of sensor [9]. AChE is considered to be the best enzyme, as it is the primary target of inhibition by metal ions in most of the metabolic pathways and holds high turnover [9].

Coupling of AChE inhibition based biosensor with nanomaterial offer distinctive advantages in terms of improved sensitivity, selectivity and lower detection limits [10]. Moreover, usage of nano-interface supports loading of large

Electronic supplementary material The online version of this article (https://doi.org/10.1007/s00604-018-2822-6) contains supplementary material, which is available to authorized users.

✉ John Bosco Balaguru Rayappan
rjbosco@ece.sastra.edu

[1] Nano Sensors Lab, Centre for Nanotechnology & Advanced Biomaterials (CeNTAB), School of Electrical Engineering, SASTRA (Deemed to be University), Thanjavur, Tamil Nadu 613 401, India

[2] School of Electrical & Electronics Engineering, SASTRA (Deemed to be University), Thanjavur, Tamil Nadu 613 401, India

[3] CSIR- Central Electrochemical Research Institute, Karaikudi, Tamil Nadu 630 003, India

[4] School of Chemical and Biotechnology, SASTRA (Deemed to be University), Thanjavur, Tamil Nadu 613 401, India

Published online: 12 May 2018

amount of AChE and promotes the redox interactions due to its inherent catalytic behavior [11, 12].

In the present work, Ru(II)-tris(bipy)-GO nanocomposite was synthesized and the same was used as a transducing element in detecting As^{3+} and Cd^{2+} ions with high sensitivity and lower detection limit. The other challenges involved in detection of As^{3+} and Cd^{2+} ions are selectivity, interference and anti-fouling. The electrocatalytic activity of Ru(II)-tris(bipy)-GO nanocomposite was proved by our group in detecting Cd^{2+}, Pb^{2+}, As^{3+} and Hg^{2+} ions simultaneously [13]. To the extent of our knowledge, for the first time Ru(II)-tris(bipy)-GO nanocomposite is being utilized as an interface material in inhibition based biosensor.

Materials and methods

Chemicals

Graphite (<20 μm size), ruthenium(II)-tris(bipyridine) chloride, hydrogen peroxide and sulphuric acid were purchased from Sigma-Aldrich, Canada (https://www.sigmaaldrich.com/canada-english.html). Citrate buffer was prepared by mixing sodium citrate, citric acid (purchased from Sigma Aldrich, India; https://www.sigmaaldrich.com/india.html) in deionized water. Acetyl thiocholine chloride, acetylcholinesterase (C2888), sodium chloride, potassium chloride, calcium chloride, phosphoric acid, ethylene diamine tetraacetic acid (EDTA), acetic acid, iron(III) chloride, lead(II) nitrate, cadmium(II)acetate, nickel(II) nitrate, cobalt(II) acetate, zinc(II) chloride, mercuric(II) sulphate, arsenic (III) iodide, potassium acetate, copper(II) chloride, dichlorvos, carbafuran and chitosan (448869) were bought from Sigma-Aldrich, India (https://www.sigmaaldrich.com /india.html). All experimental studies were carried out at room temperature using deionized water and repeated for five times to ensure the sensing characteristics.

Choice of material

Ru(II)-tris(bipy)-GO nanocomposite was utilized as an interface as it offers the advantage of high surface area for AChE to bind and enhance charge transfer rates due to π-π stacking interactions of nanocomposite [14]. Ru(II)-tris(bipy) interacts with GO to form Ru(II)-tris(bipy)-GO nanocomposite in which electrostatic interactions played a crucial role. The Ru metallic center of the co-ordination molecule interacted with COO^- and the ligand bipy molecule interacted with C=C of GO to form a stable Ru(II)-tris(bipy)-GO nanocomposite [15]. In case of nanocomposite, Ru(II)-tris(bipy) acts as a center and GO acts as a bridging ligand to allow the electron to tunnel to the working electrode from the Ru(II)-tris(bipy) center. During the electrochemical interaction, negatively charged GO attracts the arsenic and cadmium cations to the surface due to electrostatic interaction [16] and further these metal ions form a weak hydrogen bonding with Ru(II)-tris(bipy) center.

Synthesis and characterization of Ru(II)-tris(bipy)-GO nanocomposite

Ru(II)-tris(bipy)-GO nanocomposite was synthesized by chemical synthesis route reported elsewhere [17]. Modified Hummer's method was adopted to synthesize GO [18]. In the preparation of GO, 10 g of graphite was dispersed in 7.5 g of $NaNO_3$ and 621 g of H_2SO_4. The mixture was allowed to stir for 3 h and the graphite layers were exfoliated using $KMnO_4$ (45 g) in an ice bath for about 3 h. Finally 30% of hydrogen peroxide was added to stop the reaction and the mixture was centrifuged at 12000 rpm for 20 min and cleaned multiple times till pH reaches neutral. The precipitate was ultrasonicated for 1 h and aqueous brownish GO solution was collected. To prepare the nanocomposite, 10 mL of GO solution was stirred at an rpm of 800 along with 10 mg of ruthenium(II)-tris(bipyridine) chloride in 10 mL of ethanol under dark condition (Supplementary Fig. S1). Aqueous dispersion was centrifuged at 12000 rpm for 45 min and precipitate was washed thrice to remove unreacted Ru(II)-tris(bipy) and the pure form was utilized for all the experiments.

Morphological studies of Ru(II)-tris(bipy)-GO nanocomposite was examined using Field Emission Scanning Electron Microscope (FE-SEM) (Model: JSM 6701F, JEOL, Japan), Field Emission Transmission Electron Microscope (FE-TEM) (Model: JEM 2100F). Energy Dispersive X-Ray Spectroscopy (EDS) (Oxford Instruments, UK) was utilized to confirm GO and Ru(II)-tris(bipy)-GO by checking the presence of carbon, oxygen and ruthenium. Vibrational modes of synthesized Ru(II)-tris(bipy)-GO nanocomposite was deliberated using Raman Spectrometer (RENISHAW (M005–141)) with an excitation wavelength of 514 nm. The functional group analysis was studied using Fourier Transform Infrared Spectrometer (FT-IR) (Spectrum 100, Perkin Elmer, USA). Voltammetric and amperometric analysis were studied using CH analyser (CH600C, CH Instruments, USA). Atomic Absorption Spectrometer (AAS) (Perkin Elmer, Model no. 2380) was utilized to validate the observed results.

Fabrication of Pt/Ru(II)-tris(bipy)-GO/AChE electrode

Initially Pt working electrode was cleaned using 0.05 μm alumina. A homogeneous dispersion of Ru(II)-tris(bipy)-GO (0.1 g) containing100 μL of AChE (150 U mL^{-1}) was dropped on to the surface of Pt electrode and sealed with 2 μL of chitosan (0.05 wt. /v %). Chitosan surface of modified Pt electrode provides stability to nano-interface and acts as a perm-selective layer for the metal ions to interact at the electrode surface.

Electrochemical characterization and regeneration of Pt modified electrodes

Ru(II)-tris(bipy)-GO and AChE modified Pt electrodes were evaluated using cyclic voltammetry (CV), impedance analysis and amperometry. Pt/Ru(II)-tris(bipy)-GO/AChE was tested in the presence of As^{3+} and Hg^{2+} ions using amperometry. Inhibition characteristics were measured in the presence of 18 μM of ATCh, with varying metal ion concentration and the degree of inhibition (I %) was estimated using Eq. (1),

$$I\% = \left[\frac{I_0 - I_i}{I_0}\right] \times 100 \quad (1)$$

where, I_0 and I_i are the current response with and without metal ions, respectively.

Reactivation of Pt/Ru(II)-tris(bipy)-GO/AChE was studied by immersing in 0.1 M reactivator (EDTA) for 15 min. The modified electrode was washed and the reactivation was calculated using Eq. (2)

$$\text{Reactivation } (R\%) = \frac{I_r - I_{p,exp}}{I_{p,control} - I_{p,exp}} \times 100 \quad (2)$$

where, I_r is the current value of ATCh on reactivated Pt/Ru(II)-tris(bipy)-GO/AChE electrode, $I_{p,\ exp}$ is the current value of Pt/Ru(II)-tris(bipy)-GO/AChE electrode in the presence of metal ion and $I_{p,contrl}$ is the current value of ATCh on Pt/Ru(II)-tris(bipy)-GO/AChE electrode.

Results and discussion

Cyclic voltammetric study of Pt/Ru(II)-tris(bipy) -GO/AChE electrode

Voltammetric behavior of bare Pt, Pt/AChE, Pt/GO/AChE and Pt/Ru(II)-tris(bipy)-GO/AChE electrodes were studied in the potential range of −0.5 to 0.5 V in the presence of 0.5×10^3 μM $K_3[Fe(CN)_6]$ in 0.1×10^6 μM KCl (pH 6) with 1 μM of ATCh (Fig. 1a). Voltammograms were recorded with a potential sweep of 0.1 Vs^{-1}. Bare Pt electrode was electrochemically tested and no peak was observed. Modification of Pt working electrode with AChE, GO/AChE and Ru(II)-tris(bipy)-GO/AChE; exhibited reduction and oxidation peaks due to the oxidation of thiocholine in the presence of redox couple. An increased current response was observed for Pt/GO/AChE, Pt/Ru(II)-tris(bipy)-GO/AChE due to the catalytic and electrocatalytic behavior of AChE and GO, Ru(II)-tris(bipy)-GO, respectively. During the catalytic reaction, ATCh binds to the active sites of AChE and hydrolyzes to form thiocholine and acetic acid (Fig. 1b). The so formed thiocholine (RSH) in the presence of ferricyanide dissociates to form dithiobischoline (RS-SR) due to the electro redox behavior of ferricyanide. The observed redox potentials were in accordance with available reports in literature [19–21] and the redox peak parameters are shown in Supplementary Table S1.

Electrochemical impedance spectroscopic (EIS) analysis

The interfacial properties like heterogeneous charge transfer and transfer resistance of Pt modified electrodes were investigated in 0.1 μM of ATCh. Nyquist plot (Fig. 1c) of Pt/Ru(II)-tris(bipy)-GO/AChE exhibited a lower charge transfer resistance (R_{ct}) than Pt/AChE and Pt/GO/AChE (Supplementary Table S1). The curves shown in Fig. 1c represents the experimental data for bare Pt, Pt/AChE, Pt/GO/AChE and Pt/Ru(II)-tris(bipy)-GO/AChE electrodes. Heterogeneous electron transfer rate constant (K_0) and exchange current (i_0) were also estimated to choose the electrode with high catalytic activity and are presented in Supplementary Table S1.

$$i_0 = \frac{RT}{R_{ct}nFA} \quad (3)$$

$$K_0 = \frac{RT}{R_{ct}Cn^2F^2A} \quad (4)$$

where, R is constant, T is temperature, n is the number of charges transferred ($n = 2$), C is the concentration of substrate, F is the Faradaic constant and A is the area of the platinum electrode. Among the modified Pt electrodes, Pt/Ru(II)-tris(bipy)-GO/AChE showed superior characteristics in terms of current response and electron transfer rate with high electro catalytic activity [22, 23]. Hence, Pt/Ru(II)-tris(bipy)-GO/AChE electrode was chosen for further experimentation.

Effect of ATCh, arsenic and cadmium ions

The experimental parameters like electrolyte, pH, scan rate and AChE concentration were optimized and the citrate buffer with pH 6 at a scan rate of 0.1 Vs^{-1} yielded better results with an AChE concentration of 4 U mL^{-1}. Under the optimized conditions of buffer, pH, scan rate and AChE concentration, amount of ATCh concentration required for attaining maximum current response was optimized by changing ATCh from lower concentration (0.1 μM) to higher concentration (20 μM). An increased response of current was noticed with an increase in ATCh and reached a maximum saturating current at 18 μM due to the completely filled active sites of AChE. To the saturated concentration of ATCh, 1 μM of arsenic and cadmium was added in 0.1 M citrate electrolyte (Fig. 2a). On adding metal ions, a decline in current response was observed because of fully occupied active sites of AChE by metal ions via –SH linkage. Hence, conversion of ATCh to thiocholine and release of electrons at the active sites

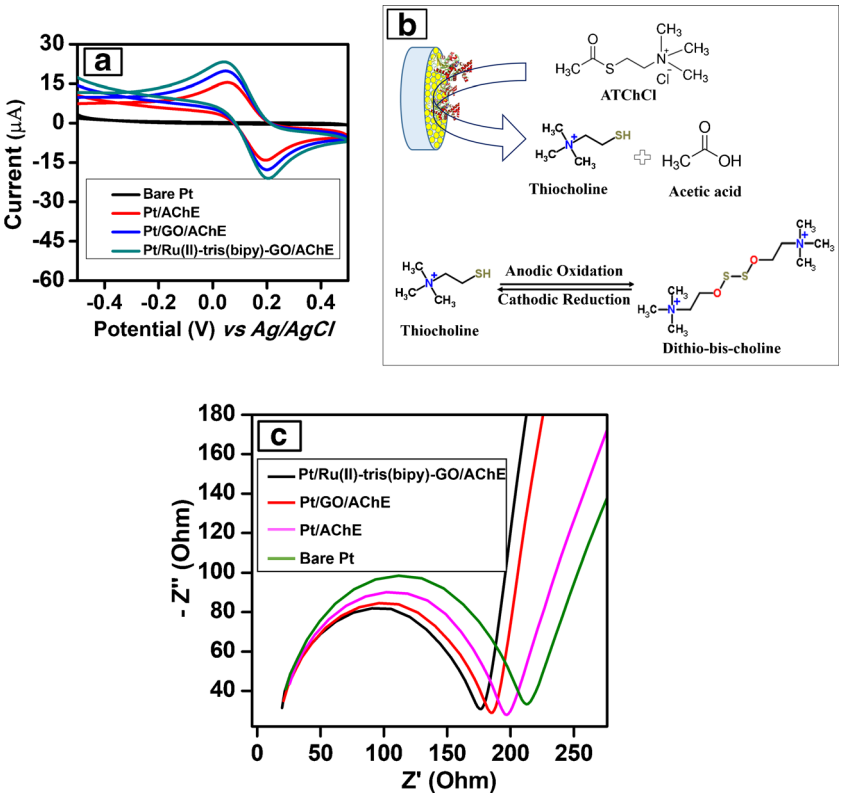

Fig. 1 **a** Cyclic voltammetric responses of various modified electrodes in the presence of 0.1 μM of ATCh and 0.5 × 10^3 μM potassium ferricyanide in 0.1 × 106 μM of KCl at a scan rate of 0.1 Vs^{-1}, pH 6; (**b**) schematic of electrochemical reaction of ATCh in the presence of AChE and (**c**) EIS analysis of various modified electrodes in the presence of 1 μM of ATCh in 0.1 M of KCl at a scan rate of 0.1 Vs^{-1}, pH 6

got restricted. Ru(II)-tris(bipy) acts as a center and GO acts as a bridging ligand to allow the electron to tunnel to the working electrode from the Ru(II)-tris(bipy)center. During the electrochemical interaction, negatively charged GO attracts the arsenic and cadmium cations to the surface due to electrostatic interaction [16] and further these metal ions form a weak hydrogen bonding with Ru(II)-tris(bipy) center. Though As^{3+} and Cd^{2+} ions exhibited inhibition effect, inhibition rate and their redox potentials were observed to be different (Fig. 2b). As^{3+} ions exhibited an oxidation peak potential at 0.214 V and Cd^{2+} ions exhibited oxidation peak at 0.223 V respectively. Hence, 0.214 and 0.223 V vs *Ag/AgCl* were utilized as amperometric input potentials for As^{3+} and Cd^{2+} ions respectively.

Amperometric inhibitive assay of arsenic and cadmium ions

Amperometric inhibitive assay of As^{3+} and Cd^{2+} ions was carried out in 0.1 M citrate electrolyte (pH 6) based on the current response of enzymatically generated thiocholine on Pt electrode at a potential of 0.214 and 0.223 V for As^{3+} and Cd^{2+} ions. Amperometric studies showed an increasing trend till 18 μM of ATCh and reached saturation in similar to voltammetric studies. At 0.214 V, addition of arsenic slowed down the thiocholine oxidation process and thus a decreased slope of the current versus time curve was observed (Fig. 2c). It exhibited a limit of detection (LOD) as 0.03 μM, sensitivity of 106.05 μA μM^{-1} cm^{-2} and a dynamic range of 0.05–0.8 μM with 94.2% of inhibition. Similar to As^{3+}, Cd^{2+}displayed an amperometric inhibitive response at 0.223 V (Fig. 2d) with a LOD of 0.07 μM, sensitivity of 124.7 μA μM^{-1} cm^{-2} and a dynamic range of 0.02–0.7 μM with 90.6% of inhibition. A calibration plot of inhibition percentage versus metal ion (As^{3+} and Cd^{2+}) concentration shows the linear equations as $I\ (\%) = -16.65\ [As^{3+}] + 58.13$, $R^2 = 0.99$ for different concentrations of arsenic (0.05, 0.10, 0.20, 0.30, 0.40, 0.50, 0.60, 0.70, 0.80, 0.90 μM) and $I\ (\%) = -19.59\ [Cd^{2+}] + 51.42$, $R^2 = 0.97$ for different concentrations of cadmium (0.02, 0.05, 0.08, 0.1, 0.2, 0.3, 0.4, 0.4, 0.5, 0.6, 0.7 μM) respectively. The analytical enactment of sensing exhibited superior characteristics in terms of selectivity towards both As^{3+} and Cd^{2+} ions, limit of detection and sensitivity. Hence, the results confirmed that Pt/Ru(II)-tris(bipy)-GO/AChE exhibited agreeable performance characteristics satisfying the WHO permissible limits in detecting As^{3+} and Cd^{2+} ions in water matrix.

The response time of As^{3+} and Cd^{2+} ions over Pt/Ru(II)-tris(bipy)-GO/AChE was estimated as 2 and 9 s, respectively. The analytical performance of Pt/Ru(II)-tris(bipy)-GO/AChE electrode was comparable with the other reported enzyme inhibition based electrochemical sensors in detecting arsenic and cadmium (Table 1). Sanllorente-Méndez et al. [4, 5] and

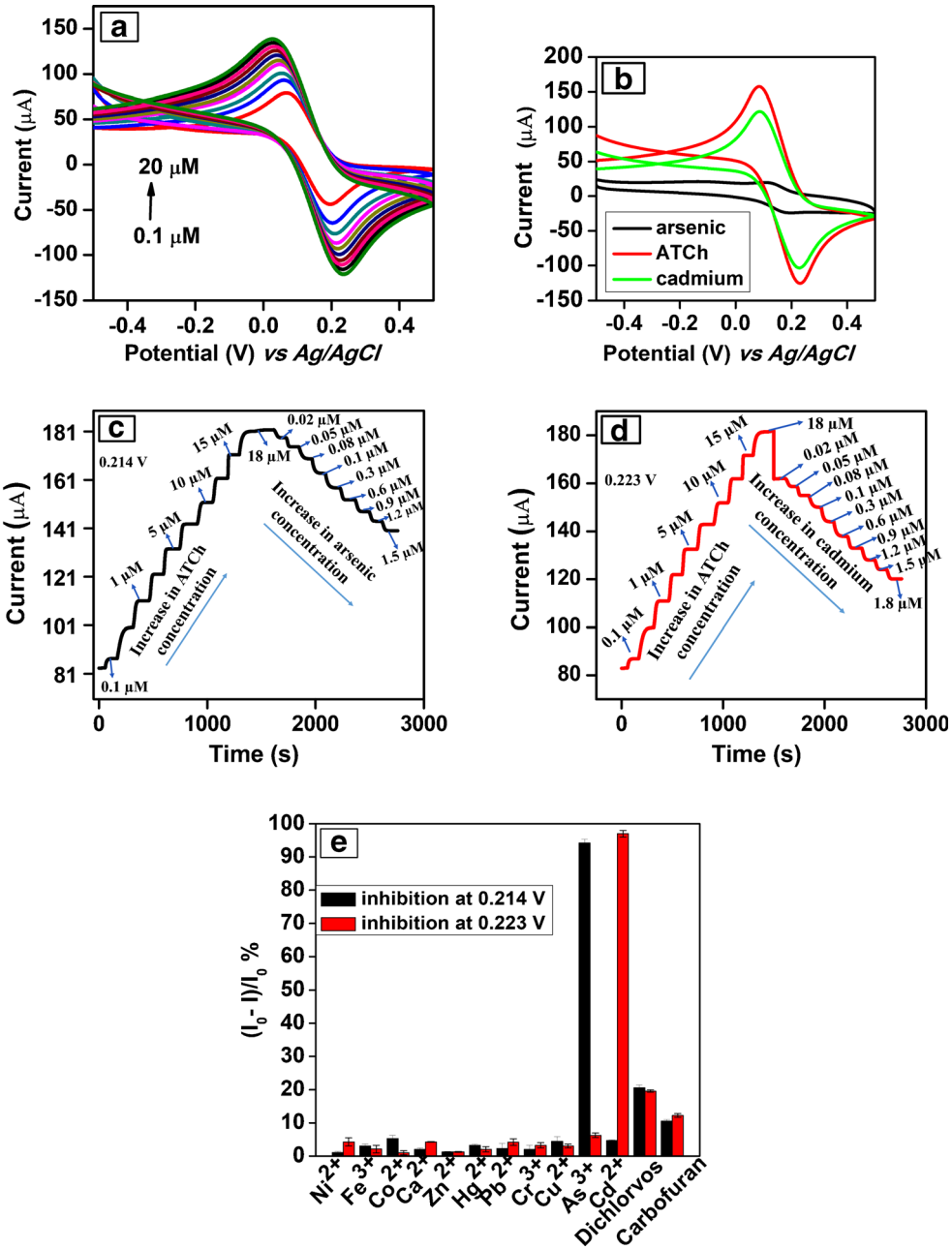

Fig. 2 Voltammetric responses of (**a**) increasing concentration of ATCh from 0 to 20 μM, (**b**) Inhibition of AChE in the presence of 18 μM of ATCh, 1.0 μM of As^{3+} and Cd^{2+} ions (**c**) Amperometric repsonses of AChE inhibition in the presence of As^{3+} at 0.214 V (**d**) Cd^{2+}at 0.223 V in 0.1 M citrate electrolyte (pH 6) and (**e**) Selectivity behavior of Pt/Ru(II)-tris(bipy)-GO/AChE electrode in the presence of interferences (0.5 μM)

Stoytcheva et al., detected As^{3+} ions using AChE modified electrodes and the electrodes exhibited a detection limit of 1.1×10^{-2} μM. However, they are limited in terms of sensitivity and linear range. The enhanced response of Pt/Ru(II)-tris(bipy)-GO/AChE might be due to the enhanced electron tunneling behavior in the presence of Ru(II)-tris(bipy)-GO nanocomposite. Ru(II)-tris(bipy)-GO nanocomposite is a conductive nanocomposite that helped in promoting the electron transfer reaction and catalyzing the electro-oxidation of thiocholine. In comparison to other works in literature, Pt/Ru(II)-tris(bipy)-GO/AChE is the only electrode with the salient features of detection limit, sensitivity and wide linear range helped in detecting both As^{3+} and Cd^{2+} ions at specific potentials.

Selectivity studies of Pt/Ru(II)-tris(bipy)-GO/AChE electrode

The selectivity of Pt/Ru(II)-tris(bipy)-GO/AChE was tested in the presence of Ni^{2+}, Fe^{3+}, Co^{2+}, Ca^{2+}, Zn^{2+}, K^{+}, Hg^{2+}, Pb^{2+}, Cr^{3+}, Cu^{2+} ions dichlorvos and carbofuran. Amperometric selectivity co-efficient (Eq. (5)), response ratio (Eq. (6)) of mixed metal ion solutions (Supplementary Table S2) were tested at 0.214 and 0.223 V for As^{3+} and Cd^{2+} ions in the presence of 0.5 μM of Ni^{2+}, Fe^{3+}, Co^{2+}, Ca^{2+}, Zn^{2+}, K^{+}, Hg^{2+}, Pb^{2+}, Cr^{3+}, Cu^{2+} ions, dichlorvos and carbofuran.

$$\text{Amperometric selectivity co-efficient } \left(K_{i,j}^{amp}\right) = \frac{\triangle I_j}{\triangle I_t - \triangle I_j} \times \frac{\triangle C_i}{\triangle C_j} \quad (5)$$

Table 1 Analytical parameters for the detection of arsenic and cadmium ions based on enzyme inhibition based biosensors

Electrode	Enzyme	Metal ion detected	LOD (μM)	Sensitivity ($\mu A\ \mu M^{-1}\ cm^{-2}$)	Linear range (μM)	Ref.
BDD/Cytochrome C electrode	Cytochrome C	As^{3+}	8.08	7.4	0–4	[24]
MWCNT/Aro/GC electrode	Arsenite oxidase	As^{3+}	8.89×10^{-3}	1.16	0–0.44	[25]
Acetylcholinesterase/SPCE	Acetylcholinesterase	As^{3+}	1.1×10^{-2}	0.068	0.01–0.1	[5]
Acetylcholinesterase/graphite electrode	Acetylcholinesterase	As^{3+}	2×10^{-4}	NM	2×10^{-4}-1×10^{-2}	[4]
Ac-MWCNTs/ Laccase	Laccase	As^{3+}	13	0.91 ± 0.07 mV/mM	$500–1.1\times10^{-4}$	[26]
GOx/PPDA/Pt	Glucose oxidase	Cd^{2+}	5	0.057	20–150	[27]
GOx/PNR/CFE	Glucose oxidase	Cd^{2+}	10.6	0.25	0.035–0.142	[28]
GOx/CoHCF/CFE	Glucose oxidase	Cd^{2+}	2.4	0.92	1.5–60	[2]
GOx/CuHCF/CFE	Glucose oxidase	Cd^{2+}	1.2	0.44	1.5–60	[2]
Interdigitated Au thin film electrode	Alkaline phosphatase	Cd^{2+}	10^{-14}	NM	NM	[29]
Platinum ultra-microelectrode with (A-G) -invertase – GOD	Invertase and Glucose oxidase	Cd^{2+}	250	NM	250–1250	[30]
Pt/PANI-co-PDTA/HRP	Horseradish peroxidase	Cd^{2+}	3.56×10^{-6}	10.016	0–88.967	[31]
Pt/Ru(II)-tris(bipy)-GO/AChE	Acetylcholinesterase	As^{3+}	0.03	106.05	0.05–0.8	Present work
Pt/Ru(II)-tris(bipy)-GO/AChE	Acetylcholinesterase	Cd^{2+}	0.07	124.7	0.02–0.7	Present work

NM = Not mentioned

BDD, boron doped diamond; MWCNT, multi walled carbon nanotubes; SPCE, screen printed carbon electrode; Aro, arsenite oxidase; GC, glassy carbon, Ac – anthracene, PPDA, poly- o-phenylenediamine, PNR, poly(neutral red), GOx/GOD, Glucose oxidase, CoHCF, Cobalt hexacyanoferrate, CuHCF, Copper hexacyanoferrate and PANI-Co-PDTA, poly(aniline-co-2,2′-dithiodianiline)

$$\text{Response ratio}\left(R_{i,j}\right) = \frac{\triangle I_j}{\triangle I_i} \quad (6)$$

where, $\triangle I_i$ is the ATCh current response, $\triangle I_j$ is the interference current response, $\triangle I_t$ is the mixed solution's current response, C_i is the metal ion concentration and C_j is the interference concentration.

Similar to As^{3+}, other interfering metal ions also showed a similar inhibition trend with the lower percentage inhibition in the orders of dichlorvos>carbofuran>$Co^{2+} > Cd^{2+} > Cu^{2+} > Fe^{3+} > Hg^{2+} > Pb^{2+} > Ca^{2+} > Cr^{3+} > Zn^{2+} > Ni^{2+}$ ions at 0.214 V. Cd^{2+} ions showed a maximum inhibition percentage at 0.223 V followed by other metal ions in the order of As^{3+} > dichlorvos>carbofuran >$Ni^{2+} > Ca^{2+} > Pb^{2+} > Cr^{3+} > Cu^{2+} > Fe^{3+} > Hg^{2+} > Zn^{2+} > Co^{2+}$ ions.

Pt/Ru(II)-tris(bipy)-GO/AChE electrode exhibited lower response ratio and selectivity coefficient in the order of 10^{-3} indicating the higher selectivity of Cd^{2+} and As^{3+} ions towards AChE. Further, the inhibition % of AChE in existence with various metal ions was estimated and represented in Fig. 2e. Lower percentage inhibition was observed for Pt/Ru(II)-tris(bipy)-GO/AChE electrode confirming that the electrode is selective in nature.

Repeatability, reproducibility and stability measurements

The reproducibility of Pt/Ru(II)-tris(bipy)-GO/AChE electrode was tested by checking the amperometric inhibition measurements of As^{3+} and Cd^{2+}ions in 0.1 M citrate electrolyte (pH 6) at 0.214 and 0.223 V, respectively. The intra-assay was verified by repeating the experiment for five times and found that the inhibition remained same with an RSD of 3.78 and 4.51% for As^{3+} and Cd^{2+} ions, respectively. The fabrication reproducibility i.e., intra-assay of Pt/Ru(II)-tris(bipy)-GO/AChE was estimated as 2.78 and 3.89% for As^{3+} and Cd^{2+} ions, respectively. Further, the stability of Pt/Ru(II)-tris(bipy)-GO/AChE was measured by testing the % inhibition of As^{3+} and Cd^{2+} ions at 0.214 and 0.223 V, respectively. During this process after each reading Pt/Ru(II)-tris(bipy)-GO/AChE was reactivated by treating with 0.1 M EDTA for about 10 min and stored at 217 K under dry conditions. Pt/Ru(II)-tris(bipy)-GO/AChE exhibited an operational stability with 21.78% loss in sensitivity at the end of 60 days. Hence, the assay is proved to be reliable.

Inhibition mechanism of AChE in the presence of As^{3+} and Cd^{2+} ions

Owing to the affinity of arsenic and cadmium towards AChE active sites and its ability to form thiol linkages with the serine of AChE, these metal ions compete with the ATCh to bind at the active sites of AChE. Hence, a study was performed to analyze inhibition type by plotting Dixon and Cornish-Bowden plots. In order to differentiate well between competitive, uncompetitive, non-competitive and mixed type of inhibition. For five varying concentrations of ATCh, Dixon plot was plotted for varying concentration of arsenic (Supplementary Fig. S5A) and cadmium (Supplementary Fig. S5B) in the range of 0.05 to 1.2 μM and 0.02 to 0.8 μM, respectively. From Dixon plots of As^{3+} and Cd^{2+} ions, it was observed to be as competitive or mixed inhibition since the five lines

Table 2 Electrochemical estimation of As^{3+} and Cd^{2+}ions using Pt/Ru(II)-tris(bipy)-GO/AChE and validation with AAS

Sample	Analyte	Added (μM)	Found (μM)	Recovery (%)	RSD	AAS
Cauvery river water	As^{3+}	1.00	1.03	103.00	4.32	ND
		2.00	2.35	117.50	2.11	ND
	Cd^{2+}	1.00	1.23	123.00	4.40	1.81 ± 0.12
		2.00	2.22	111.00	1.95	2.32 ± 0.25
Ganga river water	As^{3+}	1.00	0.98	98.00	2.15	ND
		2.00	2.15	107.50	3.15	ND
	Cd^{2+}	1.00	1.16	116.00	2.45	1.27 ± 0.12
		2.00	2.42	121.00	2.48	2.48 ± 0.24
Tap river water	As^{3+}	1.00	1.04	104.00	1.89	ND
		2.00	2.42	121.00	2.48	ND
	Cd^{2+}	1.00	1.35	135.00	3.46	1.62 ± 0.34
		2.00	2.48	124.00	1.15	2.53 ± 0.27
Waste water	As^{3+}	1.00	1.12	112.00	1.32	ND
		2.00	2.08	104.00	1.08	ND
	Cd^{2+}	1.00	1.42	142.00	2.24	ND
		2.00	2.32	116.00	1.66	ND

ND = Not determined

corresponding to the concentrations of ATCh intersect on the left of Y- axis. In order to differentiate the competitive and mixed inhibition, Lineweaver-Burk plot (Supplementary Fig. S5C and S5D) was plotted and electrocatalytic reaction is expressed as,

$$\frac{1}{I} = \frac{1}{I_{max}} + \frac{K_M}{I_{max}[S]} \quad (7)$$

where, I is the current generated due to ATCh, I_{max} is the maximum saturating current, K_M is the Michaelis-Meten constant (half of I_{max}) and [S] is the concentration of ATCh.

The I_{max} and $K_M$values in the presence and absence of arsenic and cadmium ions were presented in Table S3. I_{max} remained constant in the presence and absence of As^{3+} with an increased $K_M$confirming the competitive inhibition between As^{3+} and AChE. Cadmium exhibited a decreased I_{max} with increased K_M confirming the mixed inhibitive interactions between Cd^{2+} and AChE. The lower inhibition constant (K_i) of 1.029 and 0.39 μM for $As^{3+}$and Cd^{2+}metal ions confirms the stronger binding force that exists between metal ions and AChE. It also helps in detecting lower concentrations of inhibitors.

Real-time river and tap water sample analysis

The feasibility of Pt/Ru(II)-tris(bipy)-GO/AChE electrode for the detection of As^{3+} and Cd^{2+} ions was tested in water samples collected from river and tap. The concentrations of Cd^{2+} and As^{3+} ions in Cauvery river water collected from Thanjavur, Tamil Nadu (TDS 318 ppm, pH 6.2 and conductivity of 5.5×10^{-6} S m^{-1}); Ganga river water collected from Kolkata, West Bengal (TDS 326 ppm, pH 6.8 and conductivity of 7.2×10^{-6} S m^{-1}) tap water collected from local area (TDS 283 ppm, pH 6.2 and conductivity of 3.2×10^{-6} S m^{-1}) and waste water collected from an industrial area, Hosur, Karnataka (TDS 344 ppm, pH 3.8 and conductivity of 12.2×10^{-6} S m^{-1}) were estimated. Results were validated using AAS (Table 2). Collected water samples were filtered using a filter paper of 45 μm pore size and the same was utilized for quantification of Cd^{2+} and As^{3+} ions using standard addition method. The concentration of As^{3+} and Cd^{2+} ions in water was estimated as follows,

$$Metal\ ion\ concentration\ (\mu g/\mu L) = \frac{Current\ (\mu A) \times dilution\ factor}{slope\left(\frac{\mu A}{\mu g}\right) \times volume\ of\ diluted\ metal\ ion\ (\mu L)} \quad (8)$$

$$Recovery\ (\%) = \frac{Mean\ metal\ ion\ detected}{Metal\ ion\ added\ for\ the\ assay} \times 100 \quad (9)$$

where, dilution factor is 100 and volume of diluted metal ion used for the assay is 100 μL.

Estimated concentration of As^{3+} and Cd^{2+} ions in Ganga river water are in match with the AAS data (Table. 3). Hence, Pt/Ru(II)-tris(bipy)-GO/AChE electrode can be considered as a potential alternative to detect As^{3+} and Cd^{2+} ions in water.

Table 3 Quantification of As^{3+} and Cd^{2+} ions in Ganga river water using Pt/Ru(II)-tris(bipy)-GO/AChE and validation with AAS

Metal ion	Proposed method (μM)	AAS (μM)	Relative standard deviation (%)
As^{3+}	2.8 ± 0.23	2.21 ± 0.44	2.66
Cd^{2+}	4.4 ± 0.47	4.05 ± 0.39	3.14

Conclusion

The feasibility of Pt/Ru(II)-tris(bipy)-GO/AChE electrode was tested in quantitative estimation of As^{3+} and Cd^{2+} ions in water samples. Ru(II)-tris(bipy)-GO nanocomposite favored the immobilization of AChE and prevented enzyme fouling. The synergistic electrocatalytic behavior of nanocomposite and enzyme improved the thiocholine formation at lower oxidation potential and exhibited a better figure of merits in terms of detection limit, faster response time and sensitivity. The results demonstrated selective nature of the sensing assay in quantifying As^{3+} and Cd^{2+} ions below WHO limit. Also, the sensor was proved to be reliable in testing the real time contaminated water samples and the witnessed results are in well accordance with the results of AAS. However, the current method is limited in continuous monitoring of As^{3+} and Cd^{2+} ions due to limited activity, lower regeneration and stability of AChE.

Acknowledgements This work is supported by Department of Science & Technology, New Delhi (DST/TM/WTI/2 K14/197(a)(G)), (SR/FST/ETI-284/2011 (C)), SASTRA (Deemed to be University), Thanjavur. Dr. Manju Bhargavi Gumpu expresses sincere thanks to Science and Engineering Research Board, Department of Science and Technology for Post-Doctoral Fellowship (PDF/2017/001206).

Compliance with ethical standards The author(s) declare that they have no competing interests.

References

1. Huang M-R, Ding Y-B, Li X-G (2013) Lead-ion potentiometric sensor based on electrically conducting microparticles of sulfonic phenylenediamine copolymer. Analyst 138:3820–3829. https://doi.org/10.1039/c3an00346a
2. Ghica ME, Carvalho RC, Amine A, Brett CMA (2013) Glucose oxidase enzyme inhibition sensors for heavy metals at carbon film electrodes modified with cobalt or copper hexacyanoferrate. Sensors Actuators B Chem 178:270–278. https://doi.org/10.1016/j.snb.2012.12.113
3. Zhang H, Ding J, Du D (2015) Electrochemical evaluation of the mechanism of acetylcholinesterase inhibition based on an electrodeposited thin film. Int J Electrochem Sci 10:1632–1645
4. Stoytcheva M, Sharkova V, Panayotova M (1998) Electrochemical approach in studying the inhibition of acetylcholinesterase by arsenate(III): analytical characterisation and application for arsenic determination. Anal Chim Acta 364:195–201. https://doi.org/10.1016/S0003-2670(98)00134-2
5. Sanllorente-Méndez S, Domínguez-Renedo O, Julia Arcos-Martínez M (2010) Immobilization of acetylcholinesterase on screen-printed electrodes. Application to the determination of arsenic(III). Sensors 10:2119–2128. https://doi.org/10.3390/s100302119
6. Deshpande K, Mishra RK, Bhand S (2010) A high sensitivity micro format chemiluminescence enzyme inhibition assay for determination of hg(II). Sensors 10:6377–6394. https://doi.org/10.3390/s100706377
7. Kumar DN, Roy J, Alex SA et al (2016) Spectrofluorimetric determination of hg 2+ and Pb 2+ using acetylcholinesterase (AChE)-based formation of silver nanoparticles. RSC Adv 6:21261–21270. https://doi.org/10.1039/C6RA00193A
8. Florescu M, Badea M, Coman G, Mitrica M (2009) Screen printed electrodes used for detection of ionic heavy metals. Bull Transilv Univ Brasov 2:49–54
9. Amine A, Arduini F, Moscone D, Palleschi G (2016) Recent advances in biosensors based on enzyme inhibition. Biosens Bioelectron 76:180–194. https://doi.org/10.1016/j.bios.2015.07.010
10. Qian S, Lin H (2015) Colorimetric sensor array for detection and identification of organophosphorus and carbamate pesticides. Anal Chem 87:5395–5400. https://doi.org/10.1021/acs.analchem.5b00738
11. Chauhan N, Narang J, Jain U (2015) Highly sensitive and rapid detection of acetylcholine using an ITO plate modified with platinum-graphene nanoparticles. Analyst 140:1988–1994. https://doi.org/10.1039/c4an01873g
12. Xia N, Wang Q, Liu L (2015) Nanomaterials-based optical techniques for the detection of acetylcholinesterase and pesticides. Sensors (Basel) 15:499–514. https://doi.org/10.3390/s150100499
13. Gumpu MB, Murugan V, Krishnan UM, Rayappan JBB (2017) Simultaneous electrochemical detection of cd(II), Pb(II), as(III) and hg(II) ions using ruthenium(II)-textured graphene oxide nanocompoiste. Talanta 162:574–582
14. Dai H, Wang N, Wang D, Ma H, Lin M (2016) An electrochemical sensor based on phytic acid functionalized polypyrrole/graphene oxide nanocomposites for simultaneous determination of cd(II) and Pb(II). Chem Eng J 299:150–155. https://doi.org/10.1016/j.cej.2016.04.083
15. Murugan V, Hunter R, Neethirajan S (2015) Lipoxygenase-modified Ru-bpy / graphene oxide : electrochemical biosensor for on-farm monitoring of non-esterified fatty acid. Biosens Bioelectron 78:253–258. https://doi.org/10.1016/j.bios.2015.11.058
16. Zhao G, Li J, Ren X et al (2011) Few-layered graphene oxide nanosheets for heavy metal ion pollution management. Environ Sci Technol 45:10454–10462. https://doi.org/10.1021/ses203439v
17. Veerapandian M, Hunter R, Neethirajan S (2016) Ruthenium dye sensitized graphene oxide electrode for on-farm rapid detection of beta-hydroxybutyrate. Sensors Actuators B Chem 228:180–184. https://doi.org/10.1016/j.snb.2016.01.028
18. Veerapandian M, Lee M-H, Krishnamoorthy K, Yun K (2012) Synthesis, characterization and electrochemical properties of functionalized graphene oxide. Carbon N Y 50:4228–4238. https://doi.org/10.1016/j.carbon.2012.05.004
19. Ovalle M, Stoytcheva M, Zlatev R et al (2008) Electrochemical study on the type of immobilized acetylcholinesterase inhibition by sodium fluoride. Electrochim Acta 53:6344–6350. https://doi.org/10.1016/j.electacta.2008.04.062
20. Arduini F, Guidone S, Amine A et al (2013) Acetylcholinesterase biosensor based on self-assembled monolayer-modified gold-screen printed electrodes for organophosphorus insecticide detection. Sensors Actuators B Chem 179:201–208. https://doi.org/10.1016/j.snb.2012.10.016
21. Stoytcheva M, Zlatev R, Velkova Z et al (2009) Analytical characteristics of electrochemical biosensors. Port Electrochim Acta 27:353–362. https://doi.org/10.4152/pea.200903353
22. Du D, Chen S, Song D et al (2008) Development of acetylcholinesterase biosensor based on CdTe quantum dots/gold nanoparticles modified chitosan microspheres interface. Biosens Bioelectron 24:475–479. https://doi.org/10.1016/j.bios.2008.05.005
23. Migliorini FL, Sanfelice RC, Pavinatto A et al (2017) Voltammetric cadmium(II) sensor based on a fluorine doped tin oxide electrode modified with polyamide 6/chitosan electrospun nanofibers and

gold nanoparticles. Microchim Acta 184:1077–1084. https://doi.org/10.1007/s00604-017-2082-x

24. Fuku X, Iftikar F, Hess E et al (2012) Cytochrome c biosensor for determination of trace levels of cyanide and arsenic compounds. Anal Chim Acta 730:49–59. https://doi.org/10.1016/j.aca.2012.02.025
25. Male KB, Hrapovic S, Santini JM, Luong JHT (2007) Biosensor for arsenite using arsenite oxidase and multiwalled carbon nanotube modified electrodes. Anal Chem 79:7831–7837. https://doi.org/10.1021/ac070766i
26. Wang T, Milton RD, Abdellaoui S et al (2016) Laccase inhibition by Arsenite/arsenate: determination of inhibition mechanism and preliminary application to a self-powered biosensor. Anal Chem 88:3243–3248. https://doi.org/10.1021/acs.analchem.5b04651
27. Guascito MR, Malitesta C, Mazzotta E, Turco A (2008) Inhibitive determination of metal ions by an amperometric glucose oxidase biosensor. Sensors Actuators B Chem 131:394–402. https://doi.org/10.1016/j.snb.2007.11.049
28. Ghica ME, Brett CMA (2008) Glucose oxidase inhibition in poly(neutral red) mediated enzyme biosensors for heavy metal determination. Microchim Acta 163:185–193. https://doi.org/10.1007/s00604-008-0018-1
29. Tekaya N, Saiapina O, Ben Ouada H et al (2013) Ultra-sensitive conductometric detection of heavy metals based on inhibition of alkaline phosphatase activity from Arthrospira platensis. Bioelectrochemistry 90:24–29. https://doi.org/10.1016/j.bioelechem.2012.10.001
30. Bagal-Kestwal D, Karve MS, Kakade B, Pillai VK (2008) Invertase inhibition based electrochemical sensor for the detection of heavy metal ions in aqueous system: application of ultra-microelectrode to enhance sucrose biosensor's sensitivity. Biosens Bioelectron 24:657–664. https://doi.org/10.1016/j.bios.2008.06.027
31. Silwana B, Van Der Horst C, Iwuoha E, Somerset V (2014) Amperometric determination of cadmium, lead, and mercury metal ions using a novel polymer immobilised horseradish peroxidase biosensor system. J Environ Sci Health A Tox Hazard Subst Environ Eng 49:1501–1511. https://doi.org/10.1080/10934529.2014.937169